Seventh South African Conference on Computational and Applied Mechanics
SACAM10
Pretoria, 10–13 January 2010

AN ENHANCED MATRIX-FREE EDGE-BASED FINITE VOLUME APPROACH TO MODEL STRUCTURES

R. Suliman [a,*], O. Oxtoby [b], A. G. Malan [b] and S. Kok [c]

[a] Department of Mechanical and Aeronautical Engineering
University of Pretoria, Pretoria, 0002, South Africa.
* rsuliman@tuks.co.za.

[b] Defence, Peace, Safety and Security
CSIR, Meiring Naude Road, Brummeria, Pretoria, 0001, South Africa.
[c] Modelling and Digital Science
CSIR, Meiring Naude Road, Brummeria, Pretoria, 0001, South Africa.

Keywords: finite volume, finite element, edge-based

Abstract

This paper presents the formulation, implementation and evaluation of an enhanced matrix-free edge-based finite volume approach to model the mechanics of solids undergoing large non-linear deformations. The developed technology is evaluated via application to a number of test-cases. As will be demonstrated, the finite volume approach exhibits distinct advantages over the Q4 finite element formulation. This provides an alternative approach to the analysis of solid mechanics and allows for the possibility of using a single discretisation strategy for both the fluid and structural domain and solving the resulting set of equations using a single solution method.

1 Introduction

Traditionally, finite element methods have been extensively used for the modelling of such problems. On the other hand, for the modelling of fluid flow phenomena finite volume methods [1] have been more dominant. Both schemes can be considered as methods of weighted residuals where they differ in the choice of the weighting function. The finite element Galerkin method uses shape functions as the weighting functions and can be easily extended to higher order by using higher order polynomials for the shape functions, while the finite volume method results by choosing the weighting function as unity. Finite element methods are typically formulated in a total Lagrangrian or undeformed configuration. In contrast, finite volume methods are based on an Eulerian or updated mesh configuration, which is not optimal for solid mechanics problems. Over the last two decades a number of authors have used finite volume methods to discretise the governing equilibrium equations of elastic [2-6] and non-linear materials [7-12].

A stable and robust fluid-flow solver, based on the compact edge-based finite volume approach [13], is available. This study was undertaken to investigate whether the same edge-

based finite volume approach could be easily extended to accurately model the mechanics of solids. This is the first instance that the proposed edge-based discretisation method is applied to model solids. There are distinct advantages in applying an edge-based approach. It is applicable to arbitrary element shapes and is computationally efficient. It is also particularly well suited to shared memory parallel hardware architectures. An accurate finite volume structural solver would allow for fluid-structure interaction problems to be solved using a unified strongly coupled scheme.

Fluid-structure-interaction (FSI) constitutes a branch of Computational Mechanics in which there exists an intimate coupling between fluid and structural or solid domains; the behaviour of the system is influenced by the interaction of a moving fluid and a deforming solid structure. Examples of FSI problems include flutter in aircraft, flows in elastic pipes and blood vessels, flow induced vibrations in flexible structures and wind response in buildings. Much effort has been spent over recent years in developing FSI modelling technology [14-19]. A major aspect of FSI analysis is the coupling of the fluid and structural components. The use of the finite volume method to model structures is investigated and compared with the traditional finite element method in this work.

2 Governing Equations

The equations of equilibrium for the solid domain are given by Cauchy's first equation of motion:

$$div T_{ij} + b_i = \rho a_i \tag{1}$$

where T is the Cauchy stress (a stress measure in the deformed configuration), b is the body force in the current configuration, ρ is the density and a is the acceleration. Note that lowercase subscripts are used to denote components in the deformed configuration, while uppercase subscripts are used to denote components in the undeformed configuration.

Eq. (1) can be transformed into a total Lagrangian or undeformed formulation [20] as shown in Eq. (2):

$$Div \sigma_{iJ} + B_I = \rho_o a_i \tag{2}$$

The total Lagrangian formulation becomes important when considering non-linear elasticity problems, as one has to distinguish between the undeformed or original and deformed or current configurations. The advantage of a total Lagrangrian formulation, over an Eulerian description, is that it eliminates the need to update the mesh and re-compute edge information after each iteration. This makes it simpler and less computationally intensive. Furthermore, it eliminates the accumulated temporal discretisation error developed when using an updated mesh formulation. The Lagrangian formulation is also preferable since the constitutive behaviour of solids is often given in terms of material or referential coordinates.

Eq. (2) contains the first Piola-Kirchoff stress, σ_{iJ} (a stress measure defined in the reference configuration), which is equal to the second Piola-Kirchoff stress, S_{IJ}, multiplied by the deformation gradient, F_{iI}, as shown in Eq. (3). The deformation gradient relates infinitesimal vectors in the undeformed configuration to their counterparts in the deformed configuration.

$$\sigma_{iJ} = F_{iI} S_{IJ} \tag{3}$$

The boundary conditions for the solid mechanics problem consist of either prescribe tractions, $\bar{\tau}$, or prescribed displacements, $\bar{u}$:

$$\sigma n = \bar{\tau} \; on \partial B_t \tag{4}$$

$$u = \bar{u} \; on \partial B_u \tag{5}$$

where ∂B_t and ∂B_u are the parts of the boundary where the surface traction and displacements are applied respectively and n is the outward pointing unit normal vector.

2.1 Constitutive Equations

For a St-Venant-Kirchoff material model, Eq. (6) is the constitutive equation that relates the stress, S, to the Green-Lagrange strain, E (a strain measure in the reference configuration).

$$S_{IJ} = 2\mu E_{IJ} + \lambda E_{KK}\delta_{IJ} \tag{6}$$

where λ and μ are called the Lamè constants and are related to the elasticity modulus and Poisson's ratio.

The Green-Lagrange strain, E, is expressed in terms of displacement gradients as

$$E_{IJ} = \frac{1}{2}\left(\frac{\partial u_i}{\partial x_J} + \frac{\partial u_j}{\partial x_I} + \frac{\partial u_k}{\partial x_I}\frac{\partial u_k}{\partial x_J} \right) \tag{7}$$

3 Discretisation

In this work we propose the use of a compact vertex-centered edge-based finite volume algorithm [13] for the purposes of spatial discretisation. The advantages of this approach have been discussed above. Neglecting body forces and casting Eq. (2) in integral or weak form by integrating over an arbitrary spatial subdomain, V_m, gives:

$$\int_{V_m} \rho_o \frac{\partial v_i}{\partial t} dV = \int_{V_m} \frac{\partial \sigma_{iJ}}{\partial x_J} dV \tag{8}$$

where v represents the velocity. Noting that the control volume, V_m, is fixed in time, differentiation and integration of the temporal term are interchangeable. In addition, the density in the undeformed configuration, ρ_o is constant. We then apply Gauss' Divergence Theorem to express the spatial derivatives in terms of fluxes. Eq. (8) simplifies to:

$$\rho_o \frac{\partial}{\partial t}\int_{V_m} v_i dV = \oint_{\partial V_m} \sigma_{iJ} \cdot n_J dA \tag{9}$$

The surface integral consists of the sum over all edges, γ_{mn}, of the control volume.

$$\rho_o \frac{\partial}{\partial t}\int_{V_m} v_i dV = \sum_{\gamma_{mn} \cap V_m} \sigma_{iJ} \cdot C_{j:mn} + \sum_{\gamma_{mn}{}^B \cap V_m} \sigma_{iJ} \cdot B_{j:mn} \tag{10}$$

where C_{mn} is the edge coefficients connecting arbitrary internal nodes m and n and B_{mn} is the edge coefficient for an edge that lies along the volume boundary.

Discretising and integrating the temporal term on the left gives:

$$\rho_o \frac{v_i^{t+\Delta t} - v_i^t}{\Delta t} V = \sum_{\gamma_{mn} \cap V_m} \sigma_{iJ} \cdot C_{j:mn} + \sum_{\gamma_{mn}{}^B \cap V_m} \sigma_{iJ} \cdot B_{j:mn} \tag{11}$$

Finally, the velocity v is given by the time rate of change of displacement u:

$$\frac{Du_i}{Dt} = v_i \tag{12}$$

which in discretised form is

$$\frac{u_i^{t+\Delta t} - u_i^t}{\Delta t} = v_i^t \tag{13}$$

The set of equations are solved via a single-step Jacobi iterative scheme [21] which is implemented such as to ensure a matrix-free and robust solution.

4 Application and Evaluation

The accuracy of the proposed finite volume method is evaluated via application to a number of geometrically non-linear test problems. The results are compared against linear and non-linear finite element formulations. The plane strain assumption is used in all these 2D problems.

4.1 Uniaxial tension

The first test problem considered was that of a 2D body in uniaxial tension. The σ_{11} stress from the finite volume as well as the linear and non-linear finite element formulations are plotted against tip displacement in Figure 1. The finite volume and finite element non-linear formulations show good agreement. The stress is approximately linear for small displacements, but deviates from the linear elasticity behaviour at larger displacements. This is expected since at large displacements there is a geometric decrease in cross-section that results in an increase in stress.

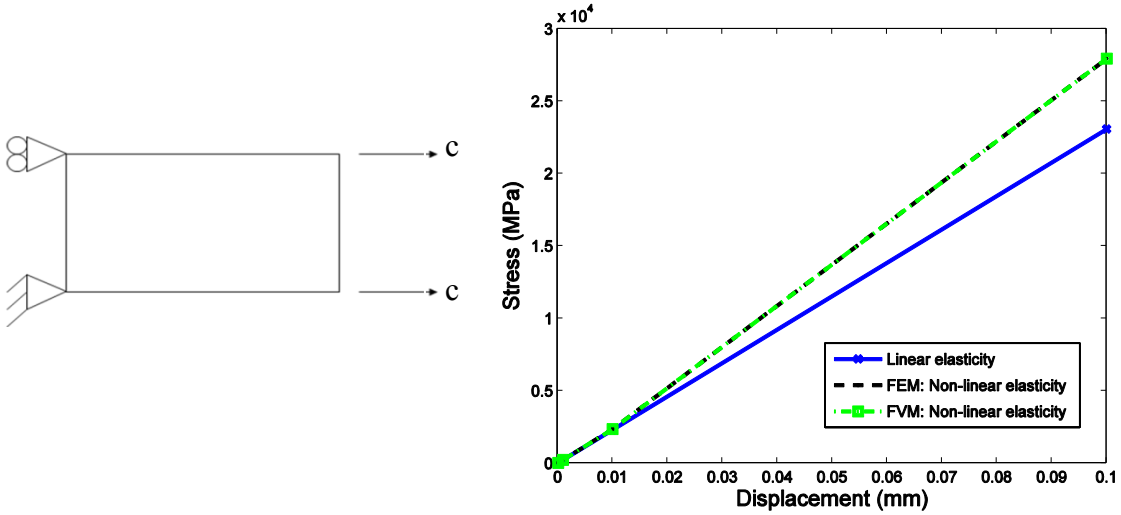

Figure 1: Comparison of stress prediction for uniaxial tension.

4.2 Simple shear

A 2D body in simple shear was considered next. Both the σ_{11} and σ_{12} stress components are plotted against tip displacement in Figure 2. Again, the finite volume and finite element non-linear elasticity formulations give exactly the same results. All the stress terms are non-zero, compared to the linear theory that only predicts a non-zero shear stress. The reason for non-zero stress terms is because the structure wants to contract in the x-direction due to the shear stress. The constraints, however, don't allow for this contraction resulting in a strain present in the y-direction, E_{22}, and because of the Poisson effect this strain results in normal stress components, σ_{11} and σ_{12}.

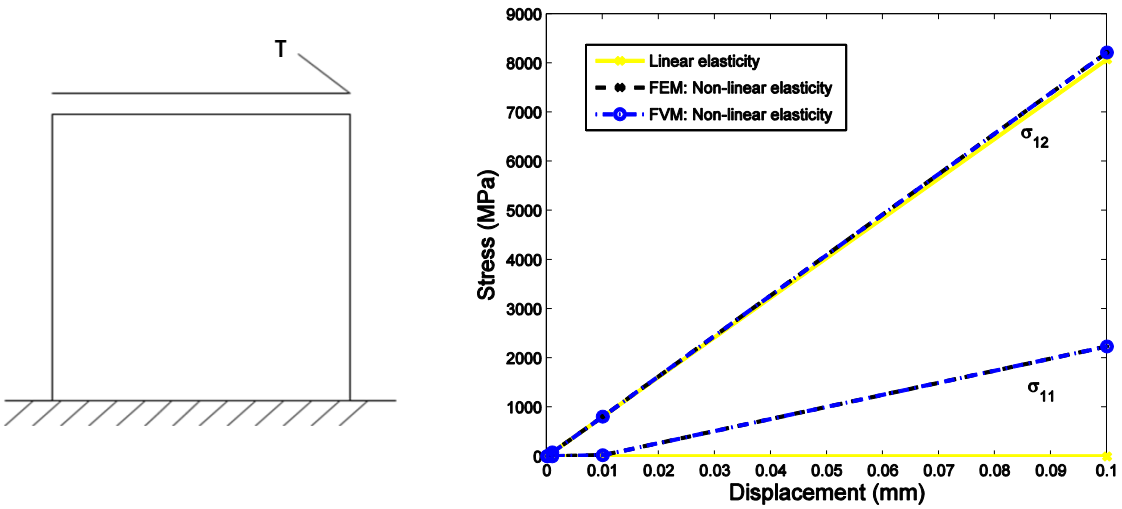

Figure 2: Comparison of stress predictions for simple shear.

4.3 Pure bending

The next problem considered was that of a thin beam in pure bending. This problem produced interesting results, as shown in Figure 3. The nodal-based formulation exhibits the undesirable characteristic of sensitivity to element aspect ratio similar to the Q4 finite element formulation. The aspect ratio is the ratio of the element's length to its width. As the aspect ratio is increased, *i.e.* the elements become long and thin, the structure becomes stiffer. This characteristic is known as locking.

To address this, an enhanced finite volume approach which uses both nodal- and elemental-strains [19] and referred to as a hybrid finite volume approach [22], was implemented. Elemental-based strains, where area integrals are evaluated at element integration points and not vertices, were used for the shear components of stress. The hybrid approach is shown to be insensitive to element aspect ratio, as can be seen in Figure 3. Furthermore, the hybrid finite volume and Q8 finite element formulations were able to predict the exact tip displacement for this problem.

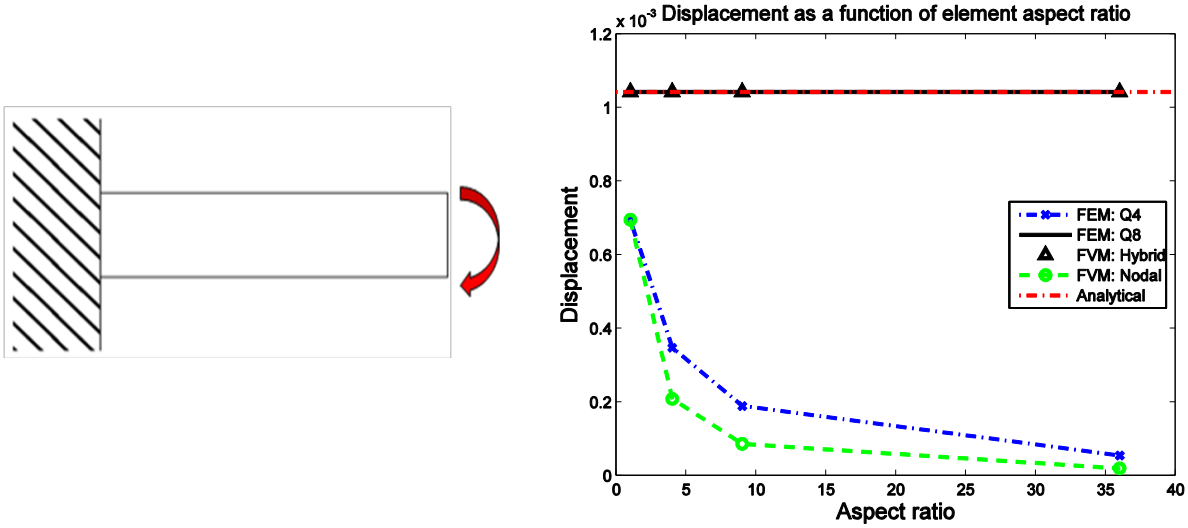

Figure 3: Displacement as a function of aspect ratio for a thin beam in pure bending.

4.4 Rate of convergence

The rates of convergence of displacements of the nodal and hybrid finite volume formulations were investigated on the problem of a thin cantilever beam subjected to a concentrated tip load. As shown in Figure 4, both formulations have a convergence rate of less than one, with the hybrid formulation being better than the nodal approach. The reason for this convergence rate was investigated analytically, by making use of Taylor series expansions and considering only the small strain case. It was found that the leading error terms are second-order accurate at internal nodes, but only first-order and zero-order accurate at boundary and corner nodes, respectively.

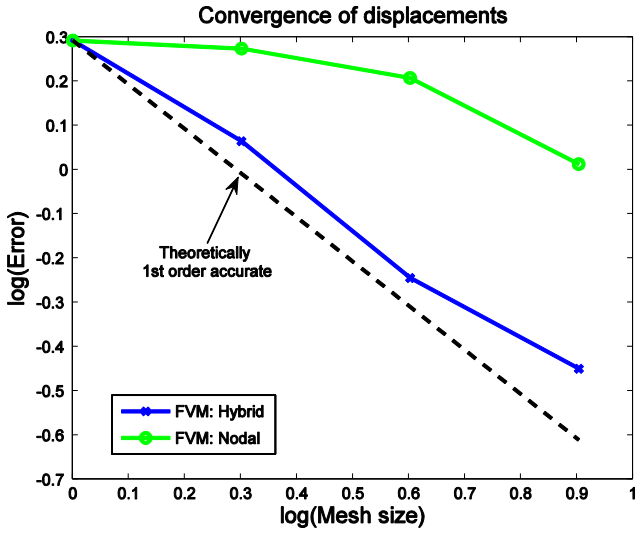

Figure 4: Convergence of displacements for the finite volume formulations.

5 Conclusion

An edge-based vertex-centered matrix-free finite volume method to model structures was investigated and compared with the traditional finite element method in this work. The finite volume method was successfully formulated and implemented in the total Lagrangian formulation. It is demonstrated that the developed technology provides exactly the same results for a simple tensile and simple shear test-case, compared with the finite element solutions. For a pure bending test-case, the standard finite volume and Q4 finite-element formulations exhibit the undesirable characteristic of sensitivity to aspect ratio. The structure becomes stiffer as the aspect ratio is increased, a characteristic known as locking. To address this, an enhanced hybrid finite volume approach which uses both nodal- and elemental-strains was implemented. The hybrid approach is shown to be insensitive to element aspect ratio, while retaining the accuracy of the nodal-strain approach. Both finite volume formulations, however, are shown to have overall displacement convergence rates of less than one.

References

1. S. V. Patankar. *Numerical heat transfer and fluid flow*, Hemisphere, Washington, DC, 1980.
2. E. Onate, M. Cervera, and O. C. Zienkiewicz. A finite volume format for structural mechanics. *Int. J. Numer. Meth. Engng*, 37:181–201, 1994.
3. I. Demirdzic and S. Muzaferija. Finite volume method for stress analysis in complex domains. *Int. J. Numer. Meth. Engng*, 37:3751–3766, 1994.
4. C. Bailey and M. Cross. A finite volume procedure to solve elastic solid mechanics problems in three dimensions on an unstructured mesh. *Int. J. Numer. Meth. Engng*, 38:1757–1776, 1995.
5. M. A. Wheel. A geometrically versatile finite volume formulation for plane elastostatic stress analysis. *J. Strain Anal.*, 31 (2), 1996.
6. M. A. Wheel. A finite volume method for analysing the bending deformation of thick and thin plates. *Comput. Methods Appl. Mech. Engrg.*, 147:199–208, 1997.
7. I. Demirdzic and D. Martinovic. Finite volume method for thermo-elasto-plastic stress analysis. *Comput. Methods Appl. Mech. Engrg.*, 109:331–349, 1993.
8. G. A. Taylor, C. Bailey and M. Cross. Solution of the elastic/visco-plastic constitutive equations a finite volume approach. *Appl. Math. Modelling*, 19:743–760, 1995.
9. N. A. Fallah, C. Bailey, M. Cross and G. A. Taylor. Comparison of finite element and finite volume methods application in geometrically nonlinear stress analysis. *Appl. Math. Modelling*, 24:439–455, 2000.
10. N. A. Fallah. A cell vertex and cell centred finite volume method for plate bending analysis. *Comput. Methods Appl. Mech. Engrg.*, 193:3457–3470, 2004.
11. P. Wenke and M. A. Wheel. Large deformation finite volume method for hyperplastic materials. *Proc. ACME'99, The Seventh Annual Conference of the Association for Computational Mechanics in Engineering, Durham, UK, 1999, pp. 113–116.*
12. K. Maneeratana and A. Ivankovic. Finite volume method for geometrically non-linear stress analysis application. *Proc. ACME'99, The Seventh Annual Conference of the Association for Computational Mechanics in Engineering, Durham, UK, 1999, pp. 117–120.*
13. A. G. Malan and R. W. Lewis. Modelling coupled heat and mass transfer in drying capillary porous materials. *Communications in Numerical Methods in Engineering*, 19(9):669–677, 2003.

14. A. K. Slone, K. Pericleous, C. Bailey, and M. Cross. Dynamic fluid-structure interaction using finite volume unstructured mesh procedures. *Computers and Structures*, 80 (5-6):371–390, 2002.
15. B. Hubner, E. Walhorn, and D. Dinkler. A monolithic approach to fluid-structure interaction using space-time finite elements. *Comput. Methods Appl. Mech. Engrg.*, 193(23-26):2087–2104, 2004.
16. C. J. Greenshields and H. G. Weller. A unified formulation for continuum mechanics applied to fluid-structure interaction in flexible tubes. *Int. J. Numer. Meth. Engng*, 64(12):1575–1593, 2005.
17. W. Dettmer and J. D. Peric. A computational framework for fluid-structure interaction: Finite element formulation and application. *Comput. Methods Appl. Mech. Engrg.*, 195(41-43):5754–5779, 2006.
18. K. J. Bathe and G. A. Ledezma. Benchmark problems for incompressible fluid flows with structural interactions. *Computers and Structures*, 85(11-14):628–644, 2007.
19. G. Xia and C.-L. Lin. An unstructured finite volume approach for structural dynamics in response to fluid motions. *Computers and Structures*, 86(7-8):684–701, 2008.
20. G. A. Holzapfel. *Nonlinear Solid Mechanics: A Continuum Approach for Engineering*, John Wiley & Sons Ltd., West Sussex, England, 2001.
21. O. C. Zienkiewicz and R. L. Taylor. *The Finite Element Method: Volume 1 - The Basis*. Butterworth-Heinemann, Oxford, fifth edition, 2000.
22. O. Oxtoby and A. G. Malan. A new unified fluid-structure interaction solver for aerospace applications. In *1st International African Conference on Computational Mechanics (AfriComp09), Sun City, South Africa, 7-11 January 2009*.